Received: 25 August 2020 | Revised: 1 April 2021 | Accepted: 6 April 2021

DOI: 10.1002/ijc.33606

MOLECULAR CANCER BIOLOGY

IJC International Journal of Cancer

Analyzing tyrosine kinase activity in head and neck cancer by functional kinomics: Identification of hyperactivated Src family kinases as prognostic markers and potential targets

Lara Bußmann[1,2,3] | Konstantin Hoffer[2,4] | Clara Marie von Bargen[5] | Conrad Droste[6] | Tobias Lange[7] | Julia Kemmling[7] | Jennifer Schröder-Schwarz[7] | Anh Thu Vu[4] | Lara Akingunsade[4] | Peter Nollau[8] | Savithri Rangarajan[9] | Rik de Wijn[9] | Agnes Oetting[1,4] | Christian Müller[6,10] | Lukas Clemens Böckelmann[7] | Henrike Barbara Zech[1] | Joanna Caroline Berger[1] | Nikolaus Möckelmann[1] | Chia-Jung Busch[1] | Arne Böttcher[1] | Fruzsina Gatzemeier[4] | Konrad Klinghammer[11] | Donjete Simnica[12] | Mascha Binder[12] | Nina Struve[4] | Thorsten Rieckmann[1,4] | Udo Schumacher[7] | Till Sebastian Clauditz[5] | Christian Stephan Betz[1] | Cordula Petersen[4] | Kai Rothkamm[4] | Adrian Münscher[1,13] | Malte Kriegs[2,4]

[1]Department of Otorhinolaryngology, Hubertus Wald Tumorzentrum, University Cancer Center Hamburg (UCCH), University Medical Center Hamburg-Eppendorf, Hamburg, Germany

[2]Laboratory of Radiobiology and Experimental Radiation Oncology, UCCH Kinomics Core Facility, Hubertus Wald Tumorzentrum, University Cancer Center Hamburg (UCCH), University Medical Center Hamburg-Eppendorf, Hamburg, Germany

[3]Department of Radiotherapy and Radiation Oncology, Hubertus Wald Tumorzentrum, University Cancer Center Hamburg (UCCH), University Medical Center Hamburg-Eppendorf, Hamburg, Germany

[4]Mildred Scheel Cancer Career Center HaTriCS4, University Medical Center Hamburg-Eppendorf, Hamburg, Germany

[5]Department of Pathology, Hubertus Wald Tumorzentrum, University Cancer Center Hamburg (UCCH), University Medical Center Hamburg-Eppendorf, Hamburg, Germany

[6]Hubertus Wald Tumorzentrum, University Cancer Center Hamburg (UCCH), University Medical Center Hamburg-Eppendorf, Hamburg, Germany

[7]Institute of Anatomy and Experimental Morphology, Hubertus Wald Tumorzentrum, University Cancer Center Hamburg, University Medical Center Hamburg-Eppendorf, Hamburg, Germany

[8]Department of Pediatric Hematology and Oncology, Research Institute Children's Cancer Center, Hubertus Wald Tumorzentrum—University Cancer Center Hamburg (UCCH), University Medical Center Hamburg-Eppendorf, Hamburg, Germany

[9]PamGene International B.V., 's-Hertogenbosch, The Netherlands

[10]Department of General and Interventional Cardiology, University Medical Center Hamburg-Eppendorf, Hamburg, Germany

[11]Department of Hematology and Oncology, Berlin, Germany

Abbreviations: DAB, 3,3′-Diaminobenzidine; DMSO, dimethyl sulfoxide; DTT, dithiothreitol; EDTA, ethylene diamine tetraacetic acid; EGFR, epidermal growth factor receptor; GST, glutathione-S-transferase; HNSCC, head and neck squamous cell carcinoma; HPV, human papillomavirus; HRP, horseradish peroxidase; IHC, immunohistochemistry; IKKβ, inhibitor of nuclear factor kappa-B kinase subunit beta; MET, mesenchymal-epithelial transition factor; MW, molecular weight; N, normal tissue; NF-κB, nuclear factor 'kappa-light-chain-enhancer' of activated B-cells; PTEN, phosphatase and tensin homologue; PI3K, phosphoinositid-3-kinase; pSFK, phospho-SFK; PMSF, phenylmethanesulphonyl fluoride; PVDF, polyvinylidene fluoride; PTK, protein tyrosine kinases; Ras, rat sarcoma; RTK, receptor tyrosine kinases; SDS-PAGE, sodium dodecyl sulfate polyacrylamide gel electrophoresis; SFK, Src family kinases; T, tumor tissue; TMA, tissue micro array; UKE, University Medical Center Hamburg-Eppendorf; WB, western blot.

[12]Department of Internal Medicine IV, Oncology/Hematology, Martin-Luther-University Halle-Wittenberg, Halle (Saale), Germany

[13]Department of Otorhinolaryngology, Marienkrankenhaus Hamburg, Hamburg, Germany

Correspondence
Malte Kriegs, Laboratory of Radiobiology and Experimental Radiation Oncology, UCCH Kinomics Core Facility, Hubertus Wald Tumorzentrum, University Cancer Center Hamburg (UCCH), University Medical Center Hamburg-Eppendorf, Martinistrasse 52, D-20246 Hamburg, Germany.
Email: m.kriegs@uke.de

Funding information
Bundesministerium für Bildung und Forschung, Grant/Award Number: 02NUK032Hamburger Krebsgesellschaft e.V.Hamburger Stiftung zur Förderung der KrebsbekämpfungMildred Scheel Cancer Career Center HaTriCS4Stiftung Tumorforschung Kopf-HalsUniversität HamburgUniversity Cancer Center HamburgUniversity Cancer Center Hamburg Research FellowshipWerner-Otto-Stiftung

Abstract

Signal transduction via protein kinases is of central importance in cancer biology and treatment. However, the clinical success of kinase inhibitors is often hampered by a lack of robust predictive biomarkers, which is also caused by the discrepancy between kinase expression and activity. Therefore, there is a need for functional tests to identify aberrantly activated kinases in individual patients. Here we present a systematic analysis of the tyrosine kinases in head and neck cancer using such a test—functional kinome profiling. We detected increased tyrosine kinase activity in tumors compared with their corresponding normal tissue. Moreover, we identified members of the family of Src kinases (Src family kinases [SFK]) to be aberrantly activated in the majority of the tumors, which was confirmed by additional methods. We could also show that SFK hyperphosphorylation is associated with poor prognosis, while inhibition of SFK impaired cell proliferation, especially in cells with hyperactive SFK. In summary, functional kinome profiling identified SFK to be frequently hyperactivated in head and neck squamous cell carcinoma. SFK may therefore be potential therapeutic targets. These results furthermore demonstrate how functional tests help to increase our understanding of cancer biology and support the expansion of precision oncology.

KEYWORDS
aberrant kinase activity, functional kinome profiling, head and neck cancer, personalized targeted therapy, Src family kinases

1 | INTRODUCTION

Head and neck squamous cell carcinoma (HNSCC) is the sixth most common cancer type with approximately 600 000 new cases diagnosed annually worldwide and a 5-year survival of 58%.[1] HNSCC is characterized by a pronounced intertumor heterogeneity, a high number of mutations and can be subdivided into human papillomavirus (HPV)-positive and HPV-negative HNSCC.[2] While viral oncogenes are the main drivers for oncogenic transformation in HPV-positive tumors, risk factors such as smoking and alcohol drive oncogenic alterations in HPV-negative HNSCC. Currently, HPV positivity is the only accepted prognostic biomarker (better prognosis) while good predictive markers are completely missing. In HPV-negative HNSCC, the most prominent alterations are the loss of heterozygosity and mutations in genes for *TP53*, *PIK3CA*, and *NOTCH1*, epigenetic changes (eg, for *CDKN2A*) and the amplification of the gene encoding the epidermal growth factor receptor (EGFR). The EGFR is of special importance in HNSCC, since this protein tyrosine kinase (PTK) is frequently overexpressed in HNSCC and anti-EGFR strategies are approved for HNSCC treatment (see below).[3,4]

The therapy of HNSCC is a prime example of multimodal treatment including surgery, radiotherapy, chemotherapy and, as mentioned above, targeted therapy. The latter includes the targeting of EGFR. However, anti-EGFR treatment has failed, especially in curative treatment,[5] presumably due to the lack of predictive biomarkers.[6] In this context, aberrant overexpression of EGFR, which could serve as a potential biomarker, is less frequent than commonly proposed while there is no good correlation between EGFR activity and its

What's new?

Protein kinases have long been thought to be important in the biology of many cancers. However, kinase expression levels don't always correlate with prognosis. Could it be kinase activity that determines tumor behavior? In this study, the authors characterized the kinome of head and neck squamous cell carcinoma (HNSCC). They found that increased activity of Src family kinases (SFK) was associated with worse prognosis, and that blocking SFK activity blocked tumor cell growth. These results indicate that functional kinome profiling may provide a valuable tool for understanding tumor biology and identifying targeted therapies.

abundance, as recently demonstrated by us.[7] In addition to EGFR, several other kinases or kinase-associated proteins such as mesenchymal-epithelial transition factor (MET), phosphatase and tensin homologue (PTEN), rat sarcoma (Ras) or phosphoinositid-3-kinase (PI3K) have been implicated in HNSCC.[2,3,8] However, discrepancies between the expression of a particular kinase and its enzymatic activity are probably not restricted to the EGFR and may therefore jeopardize efficient and personalized targeting strategies in general, not only in HNSCC. Here, functional testing is urgently needed to gain a better understanding of the molecular biology of HNSCC by identifying aberrantly activated kinases in individual patients and to fully assess their value as a target for molecular therapy.

So far, only a limited number of studies have systematically addressed the question of aberrantly activated kinases and kinase-dependent signal transduction in HNSCC. These studies used surrogate markers such as kinobeads and mass spectrometry, reverse phase microarrays or siRNA libraries.[9-11] To our knowledge, no study has systematically analyzed the kinase activity per se in HNSCC tumors, for example, via functional kinome profiling. Here we present the first comprehensive kinome profiling in HNSCC, for which PTK activity was analyzed using a functional assay. This study led to the identification of a frequent aberrant activation of Src family kinases (SFK) in HNSCC, which is associated with a poor prognosis and which may represent a target for personalized targeted therapy.

2 | PATIENTS, MATERIALS AND METHODS

2.1 | Patient samples

2.1.1 | Collection und preparation of snap frozen tissue

Biopsy specimens were sampled by experienced surgeons during diagnostic panendoscopy or during tumor surgery. The tumor and normal tissue samples were snap frozen and stored in liquid nitrogen. Time between resection and freezing was less than 60 seconds. All patients gave written informed consent. Furthermore, the ENT department has a biobank, which was notified to the Hamburg Representative for Data Protection and Freedom of Information in accordance with §12(5) HmbKHG. To enable multiple analyses from the same tissue specimen under permanently frozen conditions, the samples were subdivided and processed using two different protocols: one half of the frozen samples was smashed with a hammer (one piece was used for kinome profiling [uncontrolled lysis], another for validation experiments, a third for pathological evaluation), the other half was cut by a cryostat microtome. Here, the first and the last 5-μm slices were hematoxylin-eosin stained and used for the pathologic evaluation. The inner 300-μm slices were stored in precooled vials at −80°C and were used for kinome profiling or validation experiments (controlled lysis). However, we observed no obvious differences concerning the kinase profile or level of kinase activity between both protocols.

2.1.2 | Tissue microarray

The study retrospectively evaluated 497 cases of primary HNSCC of the oropharynx (230 cases; 108 cases were p16 negative; 74 cases p16 positive; 48 cases with unknown p16 status), larynx (170), hypopharynx (65) and the oral cavity (29). Patients had been treated at the University Medical Center Hamburg-Eppendorf (UKE), and inclusion criteria were a primary tumor treatment either by surgery or radio(chemo)therapy alone or treatment in a combined surgical and risk-based adjuvant setting. Overall survival was defined as time till death or end of follow-up. The usage of archived diagnostic left-over tissues for tissue micro array (TMA) construction and analysis for research purposes as well as patient data analysis were approved by local laws (HmbKHG, §12,1) and by the local ethics committee (Ethics Commission Hamburg, WF-049/09).

All samples were stored and analyzed at the UKE Department of Pathology. TMA construction and immunohistochemistry (IHC) have been performed as described previously.[12] Here Src (Novus Biologicals, Littleton, CO; clone: 5A18; dilution: 1:450) and phospho-SFK (pSFK, Abcam, Cambridge, UK; clone: n/a; dilution: 1:150) antibodies were used after peroxidase blocking with H_2O_2 (DAKO S2023) for 10 minutes. High-temperature pretreatment of slides was carried out in an autoclave with a citrate buffer at pH 7.8 for 5 minutes. The Envision system (DAKO 5007) was used to visualize the IHC staining. After evaluation of the staining intensity (0 to 3+) a final score was determined as described earlier.[13]

The R and Bioconductor environment[14] was used for data processing, analysis and evaluation, the R packages *survival*[15] and *survminer*[16] for survival analysis and survival curves. For the correlation analysis, *reshape2*[17] was used for data processing and the R package *corrplot*[18] for data analysis and visualization.

2.2 | Materials

2.2.1 | Substances

The substances used were SU6656 (Sigma-Aldrich, St. Louis, MO), erlotinib (Roche, Penzberg, Germany), dasatinib (Sigma-Aldrich), Saracatinib (AZD0530; Selleckchem, Houston, TX) and dimethyl sulfoxide (DMSO) (vehicle, Roche).

2.2.2 | Cells

The following HPV-negative HNSCC cell lines were obtained from Reidar Grénman (University of Turku, Turku, Finland)[19]: UT-SCC-2 (RRID:CVCL_7820), UT-SCC-5 (RRID:CVCL_7858), UT-SCC-8 (RRID:CVCL_7869), UT-SCC-14 (RRID:CVCL_7810), UT-SCC-15 (RRID:CVCL_7811), UT-SCC-16A (RRID:CVCL_7812), UT-SCC-19A (RRID:CVCL_7816), UT-SCC-19B (RRID:CVCL_7817), UT-SCC-23 (RRID:CVCL_7825), UT-SCC-24A (RRID:CVCL_7826), UT-SCC-24B (RRID:CVCL_7827), UT-SCC-29 (RRID:CVCL_7833), UT-SCC-38

(RRID:CVCL_7842), UT-SCC-42A (RRID:CVCL_7847), UT-SCC-42B (RRID:CVCL_7848), UT-SCC-49 (RRID:CVCL_7857), UT-SCC-60A (RRID:CVCL_A089), UT-SCC-60B (RRID:CVCL_A090), UT-SCC-65, UT-SCC-75 (RRID:CVCL_A092), UT-SCC-103, UT-SCC-106B (RRID: CVCL_JA24), UT-SCC-107 (RRID:CVCL_JA25), UT-SCC-108 (RRID: CVCL_JA26) and UT-SCC-113. The HNSCC cell lines Cal33 (RRID: CVCL_1108), FaDu (RRID: CVCL_1218), HSC4 (RRID: CVCL_1289), SAS (RRID: CVCL_1675), SAT (RRID: CVCL_3160), XF354/CLS-354 (RRID: CVCL_5971) have been available in the laboratory for years.[20,21]

The following cell lines are pairs: UT-SCC-19A/UT-SCC-19B, UT-SCC-24A/UT-SCC-24B, UT-SCC-42A/UT-SCC-42B, UT-SCC-60A/UT-SCC-60B, and each pair originates from the same individual. HNSCC lines and primary normal fibroblasts (F180, F184) were cultured as described recently.[7] In brief, cells were grown in Dulbecco's modified Eagle medium (Invitrogen, San Diego, CA) containing 10% FCS (PAN Biotech, Aidenbach, Germany) and 2 mM glutamine (Invitrogen) at 37°C and 100% humidification. All experiments were performed with mycoplasma-free cells. All HNSCC cell lines were recently (August 2020) authenticated using short tandem repeat profiling by Eurofins (Ebersberg, Germany). Proliferation was analyzed after 3 days of treatment using a Coulter Counter (Beckmann, Brea, CA).

2.3 | Methods

2.3.1 | Hematoxylin-eosin staining and pathological evaluation

Frozen tissue samples were fixed with 4% formaldehyde for 60 minutes, dehydrated in 25% sucrose for a total of 120 minutes and embedded in Tissue-Tek OCT, again frozen, sectioned using a cryostat microtome, thawed at room temperature, washed in phosphate-buffered saline and stained with hematoxylin-eosin using a standard protocol. Samples were dehydrated in 100% ethanol three times before being cleared two times with xylene. Samples were subsequently evaluated by an experienced pathologist and only samples which were clearly identified as normal tissue (N) or tumor tissue (T) were included.

2.3.2 | Immunohistochemistry

IHC of paraffin-embedded tissue samples was performed according to a standard protocol. Briefly, 4-μm sections were deparaffinized, pretreated with citrate buffer pH 6 for 2 × 4 minutes in a microwave, blocked with 3% H_2O_2 in methanol (after cooling), incubated with anti-pSFK (Abcam ab4816, final concentration 0.074 mg/mL) for 1 hour at room temperature, washed, incubated with biotinylated swine-anti-rabbit secondary antibody for 30 minutes, washed, complexed with a peroxidase-conjugated avidin-biotin complex and developed with 3,3′-Diaminobenzidine (DAB). Isotype controls were used instead of the primary antibody on consecutive slides. Nuclei were counterstained with Mayer's hemalum solution for 5 seconds.

2.3.3 | Kinase activity profiling

Kinase activity profiling has been described previously.[22] Here we used a PamStation12 (located at the UCCH Kinomics Core Facility, Hamburg, Germany) and PTK-PamChip arrays to profile tyrosine kinase according to the manufacturer's instructions (PamGene International, 's-Hertogenbosch, the Netherlands).[22] Whole-cell lysates were made using ~1 mm^3 of tissue and 100-μL M-PER Mammalian Extraction Buffer containing Halt Phosphatase Inhibitor and ethylene diamine tetraacetic acid (EDTA)-free Halt Protease Inhibitor Cocktail (1:100 each; Pierce, Waltham, MA). The samples were lysed for 30 minutes on ice and centrifuged afterward for 15 minutes at 16000*g* at 4°C in a precooled centrifuge. The supernatant of the lysed sample was divided in aliquots in vials precooled on dry ice and stored immediately in a −80°C freezer. Protein quantification was performed with the bicinchoninic acid assay according to the manufacturer's instructions (BCA, Sigma-Aldrich). Per array 5 μg of protein and 400 μM ATP were applied. A reduced ATP concentration (100 μM) was used for in vitro inhibition which was performed directly in the assay master mix. Technical triplicates were analyzed, and sequence-specific peptide tyrosine phosphorylation was detected by the fluorescein-labeled antibody PY20 (Exalpha, Maynard, MA) and a CCD camera using the Evolve software (PamGene International). Data were analyzed using the BioNavigator software version 5.1 (PamGene International).[22] Unless otherwise stated, data are expressed as the average signal intensity (±SD) of the 144 peptide spots based on end levels of the phosphorylation curve. Significant differences between two conditions were determined using two-sided Student's *t* test. One-way analysis of variance comparisons and Dunnett's test were applied when comparing more than two conditions.

2.3.4 | SH2-profiling

SH2-profiling was performed as described previously.[23] In brief, cell lines, tumor and normal tissue samples were pulverized by mortar and pestle under liquid nitrogen and lysed with 100 to 300 μL of lysis buffer (25 mM Tris-HCl [pH 7.4], 150 mM NaCl, 5 mM Na2EDTA [pH 8.0], 10% glycerol, 1% Triton X-100, 10 mM sodium pyrophosphate, 10 mM β-glycerol phosphate, 1 mM sodium orthovanadate, 0.1 mM freshly prepared sodium pervanadate, 1 mM dithiothreitol (DTT), 1 mM phenylmethanesulphonyl fluoride (PMSF), 1% aprotinin, 10 mM sodium fluoride). The lysate was incubated for 30 minutes on ice and centrifuged for 10 minutes at 14000 rpm at 4°C. Protein concentration was determined by Bradford-Assay according to the manufacturer's instructions (Sigma-Aldrich). An amount of 20 μg of protein extract was separated by sodium dodecyl sulfate polyacrylamide gel electrophoresis (SDS-PAGE) and blotted on a polyvinylidene fluoride (PVDF) membrane. Biotinylated SH2 domains of Src and Grb2 were purified as glutathione-S-transferase (GST)-fusion proteins from *Escherichia coli* and used after complexing with streptavidin-horseradish peroxidase (HRP) for detection as previously described.[10]

2.3.5 | Western blot

Proteins from whole-cell extracts were detected by western blot (WB) according to standard protocols. Primary antibodies anti-phospho-Src family D49G4 (Tyr416; pSFK, #6943), anti-Src L4A1 (#2110), antiphosphotyrosine pY-100 (#9411), anti-Stat3 (#4904), antiphospho-Stat3 (#9138) from Cell Signaling Technology, Inc. (Danvers, MA) and anti-ß-Actin (#A-2228) from Sigma-Aldrich, were used. Secondary antibodies were anti-mouse and anti-rabbit (Li-COR Biosciences). The Odyssey CLx Infrared Imaging System (LI-COR) was utilized for signal detection and quantification.

2.3.6 | Data evaluation

Unless otherwise indicated, experiments were repeated at least three times. The data are presented as mean values (SEM). Prism 5 software (GraphPad Software) was used for analyzing and graphing the data. The unpaired Student's *t* test was performed for the statistical analysis. *P* values were calculated using two-sided tests (*$P < .05$; **$P < .01$; ***$P < .001$). The kinome tree in Figure 3C was reproduced by the KinMap[24] and by courtesy of Cell Signaling Technology, Inc. The corrplot in Figure 3D was created with R version 3.4.1.

3 | RESULTS

3.1 | Increased SFK activity in HNSCC

To analyze the tumor-specific signal transduction in HNSCC, we sampled biopsy specimens during diagnostic panendoscopy or during tumor surgery. The samples were snap frozen immediately and stored in liquid nitrogen until further processing (Figure 1A). We collected primary tumor and corresponding normal mucosa specimens from 16 HPV-negative male patients (Table S1). Only those samples were included in the study, which were clearly identified by an experienced pathologist (Figure 1B). The PTK activity was analyzed by functional kinomics using a PamStation12. This system quantifies the phosphorylation of tyrosine-containing peptides on a corresponding microarray (Figure 1C). After quality control, which results in 123 analyzable peptides, and merging the data for all 16 patients, clear differences were observed in the signal intensities of normal (N) compared with HNSCC tumor tissue (T) (Figure 1D). The results indicate higher peptide phosphorylation and therefore higher PTK activity in tumor tissue, as confirmed by box plot analysis (Figure 1E). A two-group comparison also showed that most peptides were significantly stronger phosphorylated in the tumor fraction ($P < .05$; Figure 1F) with a more than 2-fold change (effect size [log2] fold change >1). A subsequent prediction of the relevant kinases, a so called upstream kinase analysis, predicted SFK including Src, Lck, Hck, Blk and Lyn to be significantly hyperactivated in the tumor compared with the normal tissue fraction (Figure 1G,H). In addition, MER and TXK kinases were also activated, albeit with lower specificity and significance.

We next analyzed the kinomics data for all patients individually. As shown by the heat map, differences in peptide phosphorylation were detectable in most of the patients (Figure 2A), resulting in increased overall peptide phosphorylation in the tumors (Figure 2B). Although there is variability between the patients, there was no huge variation of the mean kinase activity in the tumor group. In contrast, in the normal tissue group, the variance of the mean kinase activity was much more pronounced (Figure S2); a few normal tissue samples even showed high peptide phosphorylation comparable with the corresponding tumor (#117, 168, 175). However, increased PTK activity as shown in Figure 1D,E seems to be a general phenomenon in HNSCC and is not detected in a few samples.

The upstream kinase analysis for individual patients again revealed several upregulated members of the SFK subfamily of PTK, such as Src, Lck, Lyn, Hck, as shown exemplarily for patients #156 and #162 (Figures 3A and S1). In addition, also other PTK subfamilies were predicted to be significantly hyperactive, such as the erbB (ERB2, ERB4), the insulin receptor (IGF1R, IRR) or the ROR (ROR1, ROR2) subfamily. While upregulation of these subfamilies was predicted only for a few samples, upregulated SFK were identified in 10 of the 16 patients (Figure S1). We confirmed increased SFK activity for samples #156 and #162 using SH2 profiling and WB. While SH2 profiling uses recombinant SH2 domains for the detection of tyrosine phosphorylated proteins,[23] a Src and a pan-phospho-SFK specific antibody was used in WB experiments, the latter detecting SFK autophosphorylation. Applying an SH2 domain from Src for SH2 profiling resulted in the detection of altered Src signaling in the tumor samples compared with the normal tissue (Figure 3B). In contrast, using SH2 domain from Grb2 indicated no profound qualitative differences in Grb2-mediated signaling. WB analysis of Src expression unveiled no differences between tumor and normal tissue, the levels were comparable. Yet, the pan-phospho-SFK antibody (used as a surrogate marker for SFK activity) detected higher SFK autophosphorylation in the tumor (Figure 3C). Similar results were obtained for patients #81, 95, 130 and 168, confirming increased SFK autophosphorylation in these samples (Figure S3). As already suggested by the upstream kinase analysis, this increased SFK phosphorylation is likely not restricted to Src but may also affect other SFK members. An increased activation of SFK members with a molecular weight (MW) greater than Src (isoform 1 MW: 59.8 kDa), such as Yes1 (MW: 60.8 kDa) or Lck isoform 3 (MW: 61.2 kDa; see Table S2), is also indicated in Figure 3C, which unveils pSFK signals >60 kDa.

For SH2 profiling and WB experiments, we used comparable amounts of protein but refrained from using actin as a loading control since normal and tumor samples might differ significantly with respect to actin, while other proteins might be expressed more or less equally (Figure S4[25];). However, to validate increased SFK activity also in situ, we performed IHC, analyzing the SFK autophosphorylation. As

representatively shown for patient #81, we could indeed demonstrate increased pSFK staining in eight tumors compared with their normal epithelial tissue (Figure 3D). Furthermore, we detected increased pSFK in two additional samples which had not shown increased SFK activity so far (#151, 180). For sample #118 we confirmed the absence of increased SFK activity, while for four patients there was insufficient material for validation experiments. A summary of all these results is shown in Figure 3E.

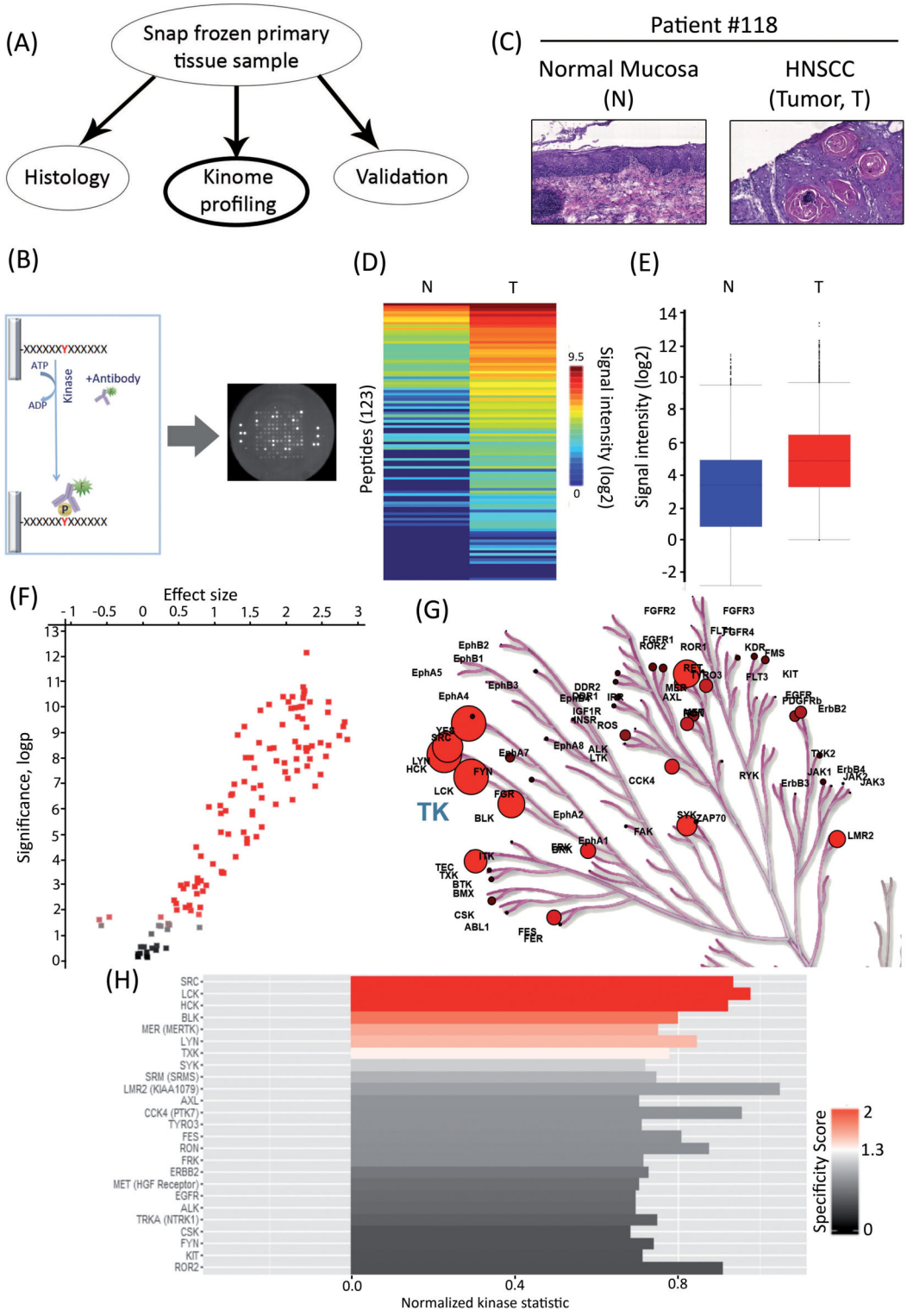

FIGURE 1 Legend on next page.

3.2 | SFK autophosphorylation and patient survival

The data presented so far indicate frequent upregulation of SFK in HNSCC. To verify this finding and to analyze a possible correlation of increased SFK activity with overall patient survival, we next analyzed Src expression and SFK autophosphorylation using a TMA including approximately 500 HNSCC samples and exemplary normal oral tissue. While normal mucosa displayed moderate staining signals we observed a remarkable variation in the HNSCC samples, encompassing no, weak, moderate or strong signals (staining intensity 0, 1, 2 and 3, respectively; Figure 4A). All oropharyngeal samples were also tested for p16 as a surrogate of HPV-dependent tumorigenesis (data not shown). Only p16-negative (and therefore HPV-negative) oropharyngeal, hypopharyngeal and laryngeal tumor samples and tumor samples from the oral cavity from patients treated with any kind of *radiotherapy* or *radiochemotherapy* were included in the analysis.

For survival analysis, we scored the staining by combining signal intensity and stained area in accordance to Simon et al.[13] There was a good correlation of this score and the staining intensity (Figure 4B) while we observed no correlation between expression of Src and SFK autophosphorylation in the patient samples (Figure 4B). Such a discrepancy is already indicated by the WB data in Figure 3C.

We observed no difference in the overall survival of patients with negative/weak/moderate vs strong (44% of the cases) Src score (Figure 4C). In contrast, strong SFK autophosphorylation (84% of the cases) was associated with significantly reduced 5-year survival rates of approximately 83% for the negative/weak/moderate pSFK group vs approximately 59% for the strong pSFK group (Figure 4D).

These data demonstrate that SFK autophosphorylation/activity is a prognostic biomarker in HNSCC, whereas analyzing only the expression of individual SFK members such as Src seems to have no prognostic relevance.

3.3 | Targeting of SFK in HNSCC cells

We next asked if SFK may be a therapeutic targets in HNSCC. To this end, we inhibited SFK in vitro by adding the pan-SFK inhibitor SU6656 to the lysates of samples #156 and #162 and performed subsequent kinome profiling. EGFR was inhibited as a negative control using the small-molecule inhibitor erlotinib. As shown in Figure 5A, SU6656 reduced overall peptide phosphorylation, demonstrating reduced overall kinase activity in the samples. While changes induced by SU6656 were more pronounced for sample #162, erlotinib treatment showed much less effect in both lysates. Further analysis of the individual peptide phosphorylation clearly demonstrates that SU6656 caused a significant reduction in phosphorylation of a majority of the peptides, while the reduction due to erlotinib treatment was much lower (Figure 5B). While these data also validate that SFK activity contributes significantly to the elevated kinase activity in the tumor samples, they also indicate that SFK inhibition could be an effective strategy to target HNSCC with upregulated SFK. The latter was verified using two clinically relevant Src/SFK inhibitors, namely, dasatinib and saracatinib. For both small-molecule inhibitors, we observed a reduction in kinase activity which was comparable with that achieved by SU6656 (Figure S5).

To test if SFK inhibition could be an effective strategy to target HNSCC with upregulated SFK, we first screened 31 HNSCC cell lines for basal SFK autophosphorylation. We observed frequent hyperphosphorylation compared with normal fibroblasts (Figure 6A) and found—in contrast to the TMA data—a moderate association ($R^2 = .55$) between Src expression and SFK activity (-Figure S6), which might be due to differences between cultured cells and primary tumor tissue. Targeting SFK by SU6656 in cells with a high pSFK level (UT-SCC 19A) caused a clear reduction in SFK-dependent signaling, demonstrated by inhibited autophosphorylation of SFK and reduced STAT3 phosphorylation (Figure 6B). For cells with weak basal SFK autophosphorylation (UT-SCC 2), only moderate effects were observed. In line with this result, cell proliferation was efficiently blocked by SU6656 in UT-SCC 19A cells in comparison with UT-SCC 2 cells or normal fibroblasts (Figure 6C). By analyzing additional cell lines, we could observe a significant correlation between basal SFK autophosphorylation and SU6656 sensitivity, with cells expressing more pSFK being more sensitive ($P = .012$, $R^2 = .68$; Figure 6D), which indicates that SFK inhibition could be a therapeutic option to treat HNSCC with upregulated SFK.

FIGURE 1 Increased protein tyrosine kinases (PTK) activity in head and neck squamous cell carcinoma (HNSCC) tumor samples compared with the corresponding normal tissue (merged data). A, Sample preparation: frozen samples were subdivided for histology, kinome profiling and validation experiments such as SH2-profiling and western blot (WB). B, Representative hematoxylin-eosin staining of normal mucosa (N) and HNSCC tumor (T) tissue (patient #118; ×100 magnification). C, Main principle of functional kinome profiling: The PamChips contain multiple copies of individual peptides. Sequence-specific tyrosine phosphorylation is detected by fluorochrome-coupled phospho-specific antibodies and CCD camera. D-G, Kinome profiling of 16 HNSCC (T) and corresponding normal mucosa (N). The data from all 16 patients were merged. D, Heatmap showing log2-transformed signal intensities for 123 phosphorylated peptides. The signals were sorted from high (red) to low (blue) intensity/phosphorylation. E, Box plots summarizing the log2-transformed signal intensity for the tumor and normal tissue group. F, Changes in peptide phosphorylation analyzed by a two-group comparison (T vs N) depicted as a volcano plot (effect size >0: higher phosphorylation in T; significance score (log2) >1.3 indicates significant changes, dotted line). G, Upstream kinase analysis of T vs N (Normalized kinase statistic (log2) >0: higher kinase activity in T; specificity score (log2) >1.3; white to red bars: statistically significant changes). H, Kinome tree highlighting kinases that were upregulated in tumor tissue. Data taken from G. The size of the circles represents the specificity score. Illustration reproduced courtesy of Cell Signaling Technology, Inc. (www.cellsignal.com)

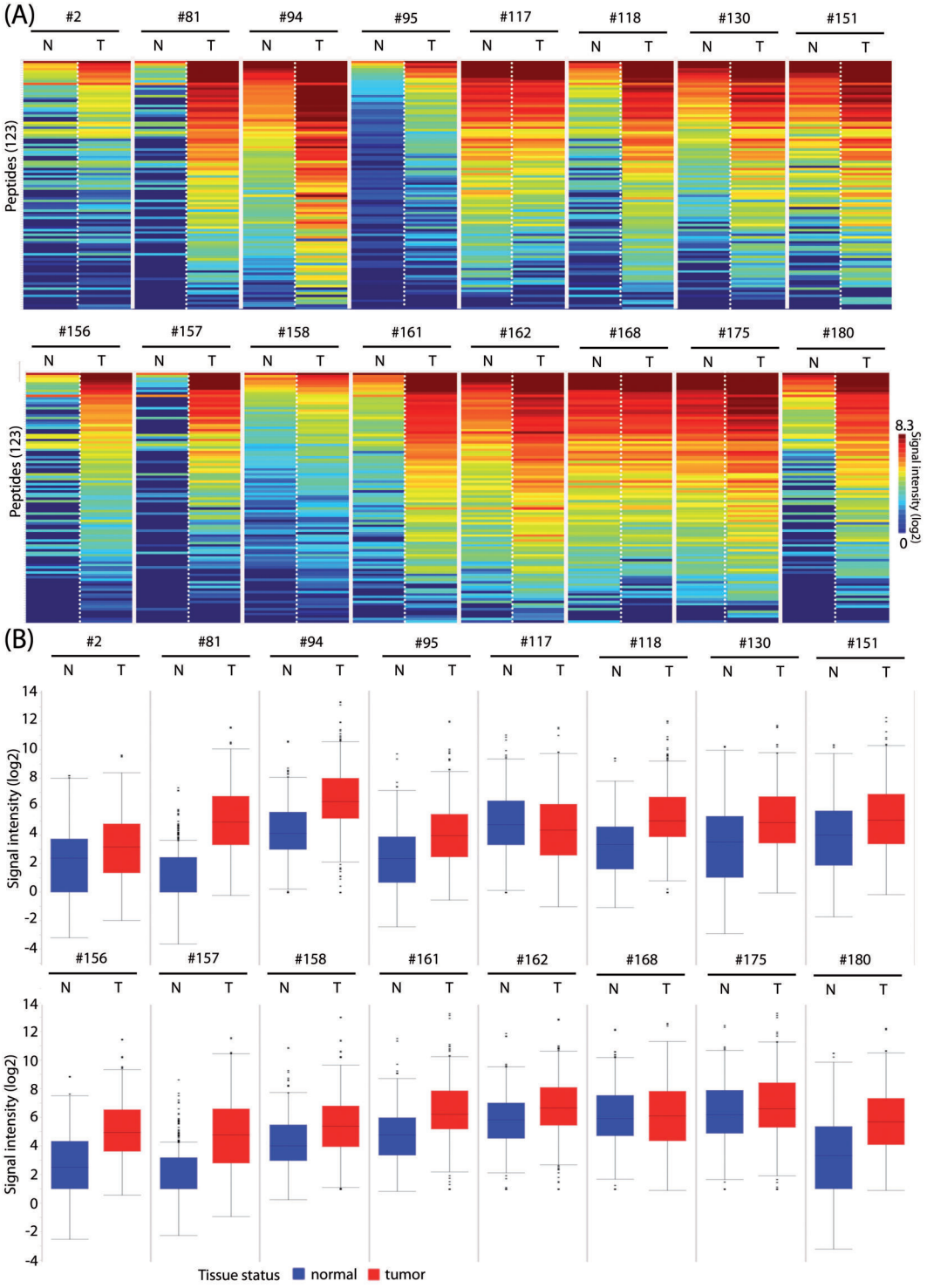

FIGURE 2 Increased protein tyrosine kinases (PTK) activity in head and neck squamous cell carcinoma (HNSCC) tumor samples compared with the corresponding normal tissue (induvial analysis). Functional kinome profiling. A, The log2-transformed signal intensities for each patient are depicted in the heatmap. The signals were sorted from high (red) to low (blue) intensity/phosphorylation. B, Box plots summarizing the log2-transformed signal intensities (peptide phosphorylation levels) of tumor and normal tissue samples per patient (data taken from A)

4 | DISCUSSION

This study presents the first systematic functional kinome analysis of patient-derived HNSCC samples at the level of PTK activity. By comparing the tumor with the corresponding normal tissue samples, we showed increased PTK activity in 13 out of 16 tumors. Subsequent upstream analysis identified several PTK as aberrantly activated in the tumors, especially members of the SFK subfamily. Furthermore,

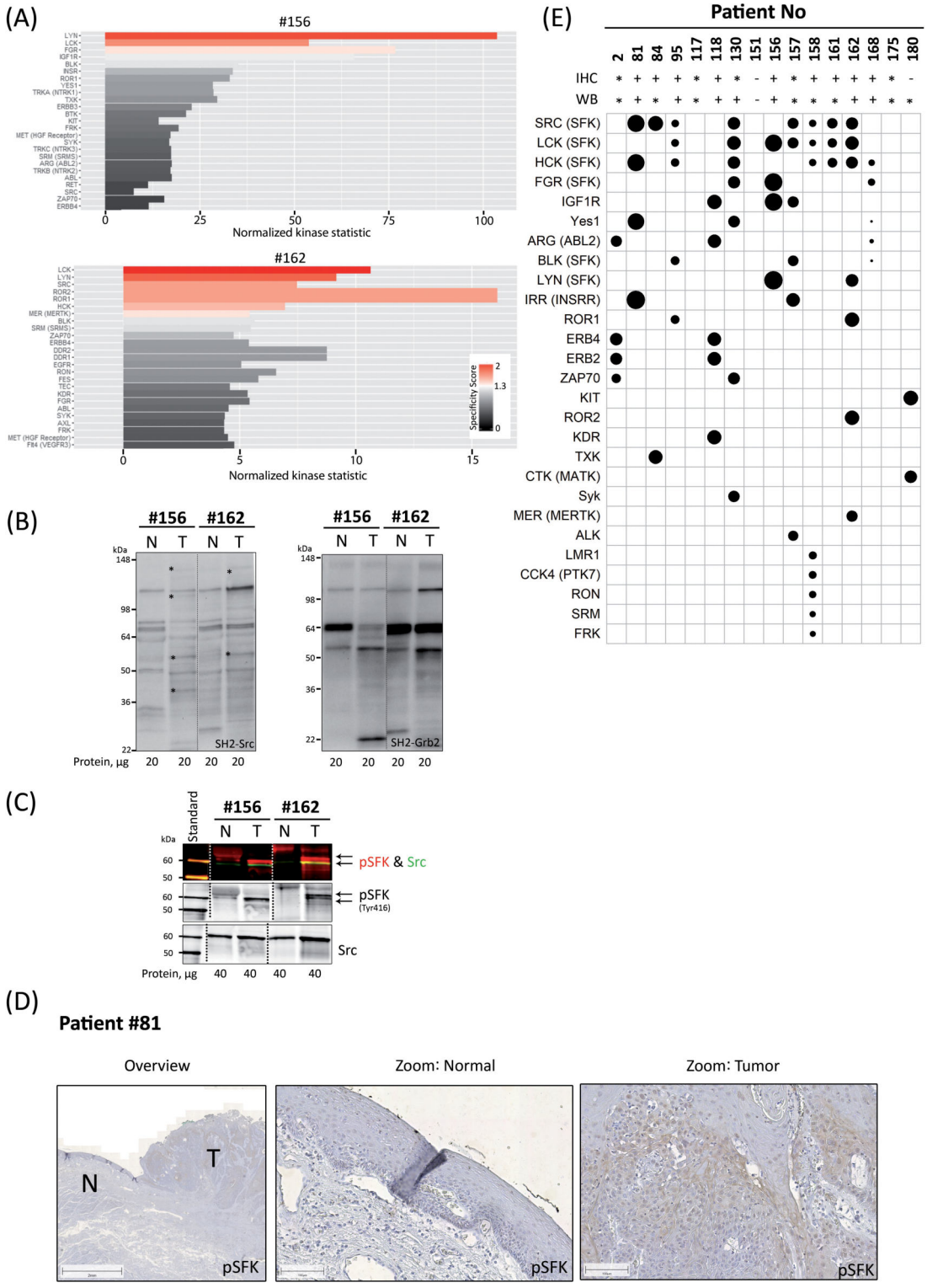

FIGURE 3 Validation of increased Src family kinases (SFK) activity in individual head and neck squamous cell carcinoma (HNSCC). Verification of increased SFK activity exemplarily shown for samples obtained from patients #156, 162 or 81. A, Upstream kinase analysis of T vs N showing the top 25 ranked kinases (normalized kinase statistic (log2) >0: higher kinase activity in T; specificity score (log2) >1.3; white to red bars: statistically significant changes). B, SH2-profiling using the SH2 domains of Src and Grb2, respectively. For all samples, 20 µg of whole-cell lysates were loaded. C, Western blot (WB) analyses detecting Src expression and SFK autophosphorylation (pSFK) in tumors and normal tissue (40 µg per lane). Overlay shows Src in green and pSFK in red. D, Immunohistochemistry (IHC) staining of pSFK (Tyr416, red) in tumor and normal tissue samples from patient #81 (scale bares as annotated). E, Summary of the kinomics and validation data. Upstream kinase analysis of T vs N depicted as a corrplot including those kinases that were significantly activated in the tumor samples (specificity score (log2) >1.3). The size of the circle indicates the normalized kinase statistic (see Figure S1). Also included are the results for the validation of the findings regarding SFK using either WB or IHC (+, results confirmed; −, results not confirmed; *, validation not possible)

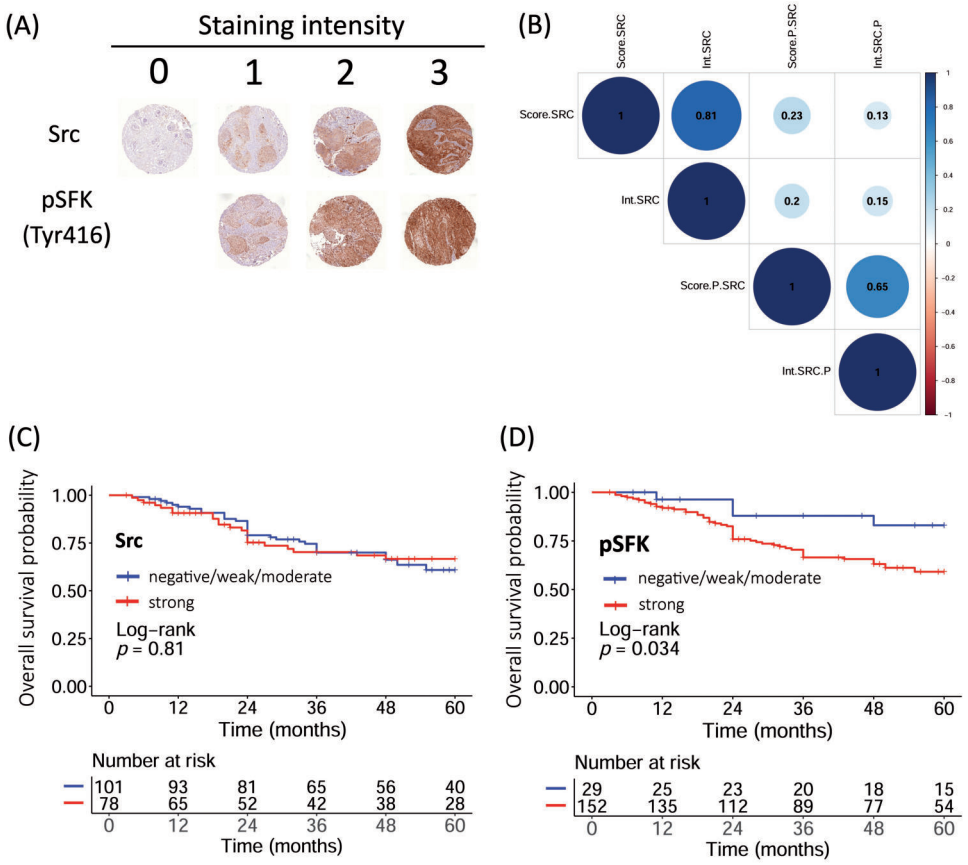

FIGURE 4 Src expression, Src family kinases (SFK) autophosphorylation and overall survival of head and neck squamous cell carcinoma (HNSCC) patients. The expression of Src and the autophosphorylation of SFK (pSFK) in human papillomavirus (HPV)-negative HNSCC patients was analyzed using a tissue micro array. A, Detection and classification of Src expression and SFK autophosphorylation. B, Circle plot showing the correlation between Src expression and SFK autophosphorylation (inten: signal intensity; score: staining scoring factor). C,D, Kaplan-Meier estimates (overall survival) of HPV-negative HNSCC patients stratified by either (C) Src expression or (D) SFK phosphorylation

we could show that increased SFK activity is frequent in HNSCC and associated with a poor prognosis. Therefore, upregulated SFK activity may be a promising target in personalized HNSCC therapy, a hypothesis which is supported by the targeting experiments using selected HNSCC cell lines.

Only the analysis of SFK activity either by functional kinome profiling or by SFK autophosphorylation made these findings possible. The analysis of only the expression of, for example, Src would not have revealed any differences between normal and tumor tissue (see Figures 3C and S3) or unveiled any clinical impact (see Figure 4C). Together with the lack of correlation between Src expression and SFK autophosphorylation in the TMA (Figure 4B)—this might also be explained by an activation of additional SFK members, which were detected by the anti-pSFK but not the anti-Src antibody—our data indicate a discrepancy between expression and activity of SFK, as also recently shown by us for the EGFR.[7] These discrepancies strongly argue for the use of functional tests for target identification as well as therapy individualization in molecular oncology. Such functional tests would have to detect more or less all SFK members in order to be used as predictive biomarkers, since our data indicate that aberrant SFK activation includes several members of this PTK subfamily. Therefore, again, either kinome profiling or pan-pSFK antibodies seem to be useful.

Src itself is one of the first discovered oncogenes and, together with other SFK members (summarized in Table S2), has been described to be upregulated in various cancer entities, controlling vital processes, such as proliferation, migration or apoptosis.[26-28] However, little is known about SFK in HNSCC. So far, Src or pSFK have not been considered prognostic in this entity. Since SFK are rarely mutated, deregulation can only be detected by studying expression or activity.[26] Consequently, hyperactive SFK were not identified in recent HNSCC studies on the genomic level[2,29] and were not considered to be of significant relevance in HNSCC development so far.[3,4] However, the high prevalence of SFK hyperactivity reported here clearly indicates an important role in HNSCC biology with possible clinical implications. This hypothesis is supported by two IHC studies showing increased expression of either Src[30] or Lyn[31] in the tumor tissue of HNSCC patients, while there was almost no expression in the adjacent normal tissue and in control epithelium. Furthermore, expression of Lyn was increased in some HNSCC cell lines as identified by chemical proteomics,[10] and siRNA screens identified Fyn to be essential for HNSCC survival.[11] Reasons for increased SFK activity can be diverse, since SFK activity can be controlled by G-protein coupled receptors, integrin signaling and several receptor tyrosine kinases (RTK).[28] Such increased RTK activity might be causative for the upregulated SFK activity observed here, since elevated RTK activity was also detected in some of the samples (eg, insulin receptor or ERBB subfamily). However, the detailed mechanisms leading to increased SFK activity in HNSCC have to be analyzed in the future. However, it is already becoming apparent that SFK signaling in

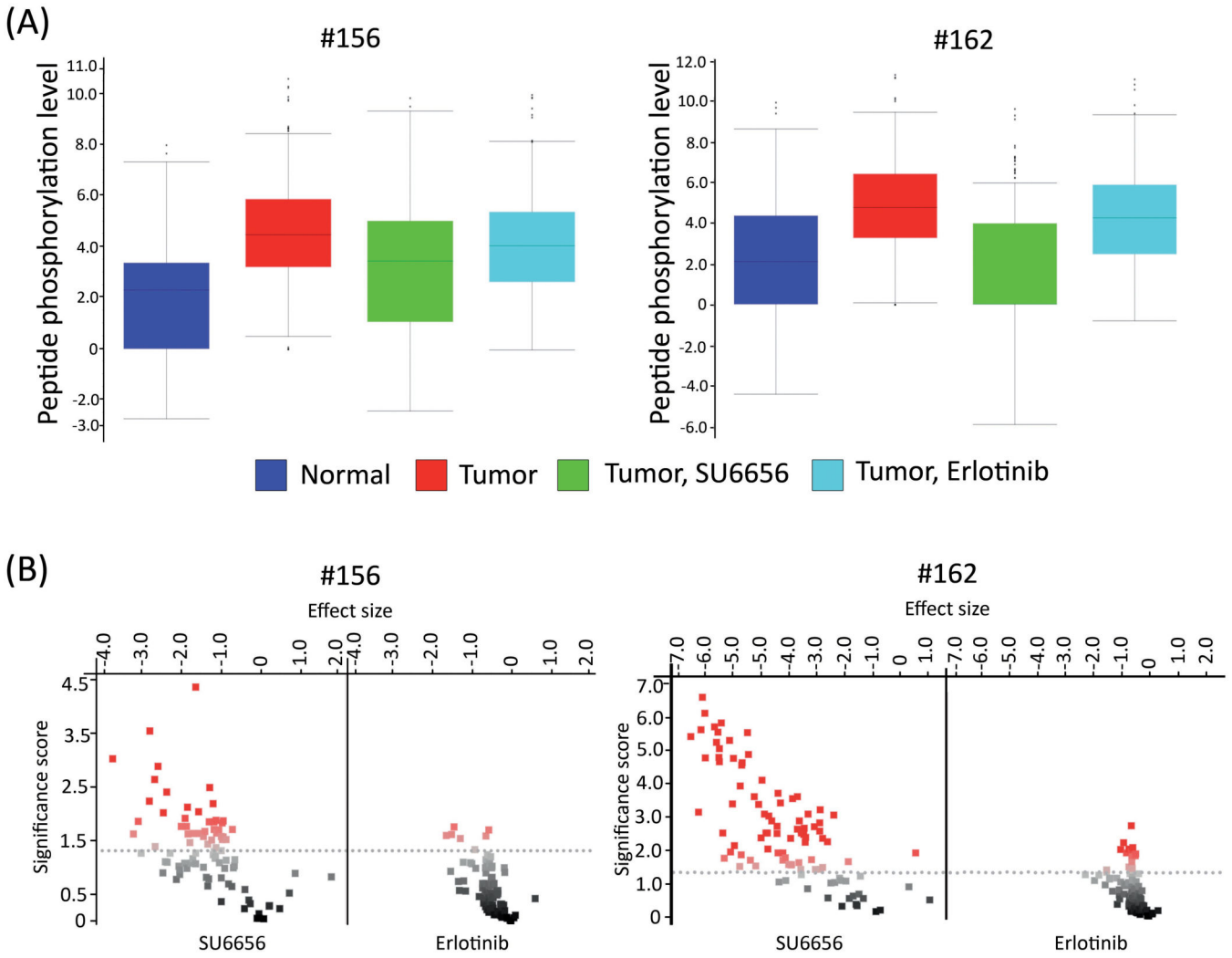

FIGURE 5 In vitro inhibition of Src family kinases (SFK). A, In vitro treatment of tumor lysates of patients #156 and #162 with 1.3 μM SFK inhibitor SU6656 or 5 μM epidermal growth factor receptor (EGFR) inhibitor erlotinib immediately before performing the functional kinome profiling. Box plot summarizing the overall peptide phosphorylation levels of the different samples per patient. B, Two-group comparison (*t* test) depicted as a volcano plot (effect size(log2) >0: higher phosphorylation in T; significance score (log2) >1.3 indicates significant changes, dotted line)

HNSCC is more complex than expected. For example, initial experiments on downstream signaling already show that increased SFK activation is not necessarily associated with increased activity of downstream targets such as STAT3 or ERK1/2 (Figure S7). Such findings will be the occasion to reconsider our understanding of signal transduction in (head and neck) cancer.

SFK inhibitors have already been approved for cancer therapy and SFK inhibition blocked proliferation especially for HNSCC cells with increased SFK activity in our study. This is in line with other studies reporting antiproliferative, antimigratory and pro-apoptotic effects after Src-inhibition in HNSCC.[31-35] However, in small studies with unselected patient cohorts, the unspecific Src inhibitors dasatinib and saracatinib did not show any clinical benefit so far, whether used alone[36,37] or in combination with erlotinib.[38]

Importantly, though, in addition to the pSFK the HPV status seems to be of relevance, too: While increased SFK autophosphorylation is associated with poor prognosis of HPV-negative (p16−), patients with HPV-positive (p16+) HNSCC and increased pSFK showed a trend towards prolonged survival (Figure S8A). This observation indicates a distinct influence of upregulated SFK in HPV-positive vs HPV-negative HNSCC and leads to the elimination of any prognostic effect when both cohorts are considered together (Figure S8B). Therefore for future studies we would definitely suggest an individualization of SFK inhibitor treatment, using SFK activity as well as HPV status as potential predictive markers. Furthermore, a combination of SFK inhibitors with radiotherapy or chemotherapy may be promising,[39-41] as well as the combination of SFK inhibitors with immune checkpoint inhibition[42] or nanotechnologies.[43,44] The intertumor heterogeneity in SFK activity should also favor the use of SFK—rather than Src-specific inhibitors; however, clinically relevant Src inhibitors are already quite unspecific—therefore, this approach should be eminently feasible for clinical studies. Moreover, compensatory mechanisms have been reported in response to SFK inhibition, which again argue for

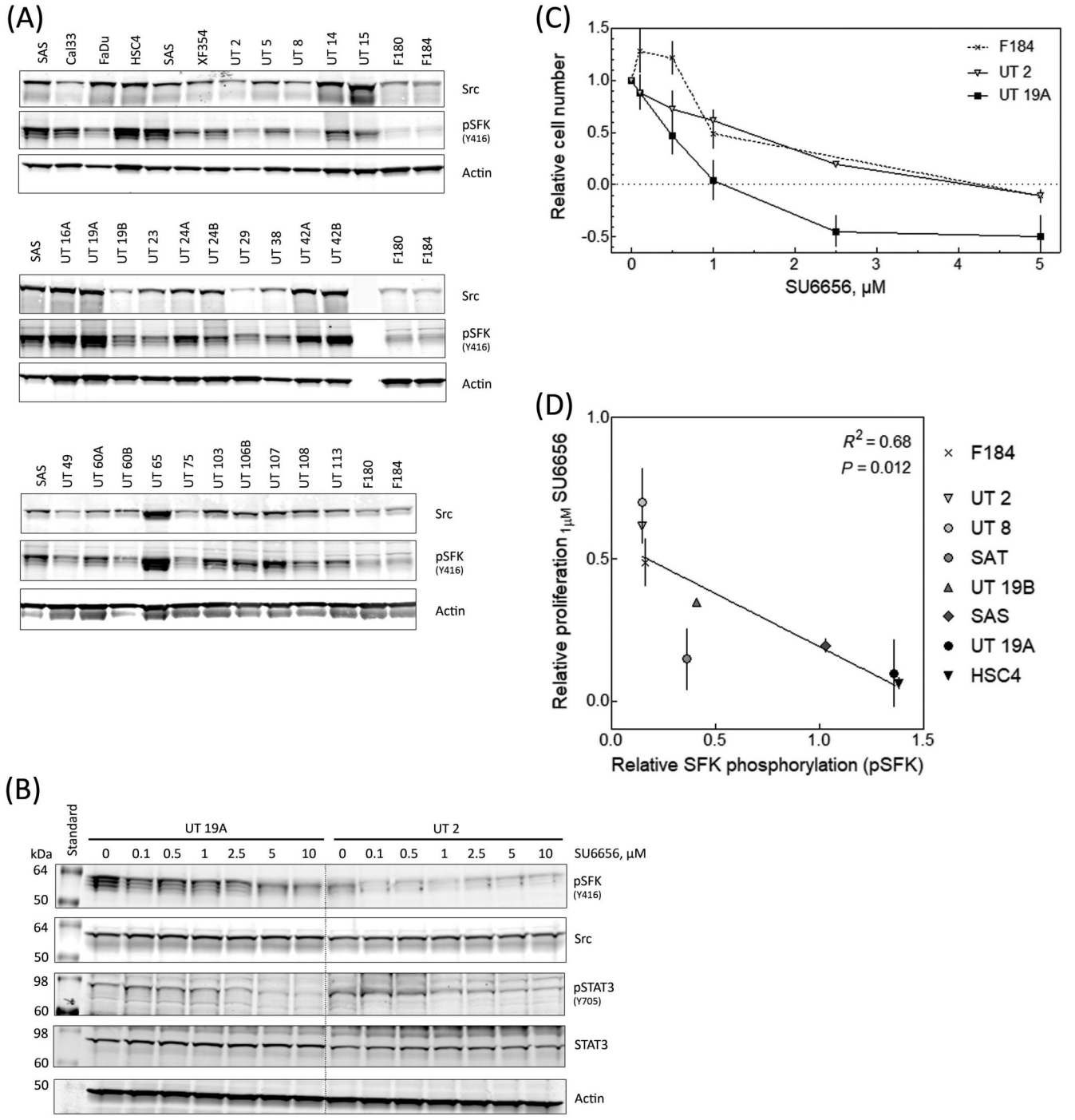

FIGURE 6 Increased Src family kinases (SFK) activity in HNSCC cell lines and impaired proliferation after SFK-targeting. A, Screening of 32 head and neck squamous cell carcinoma (HNSCC) cell lines for Src expression and SFK autophosphorylation using corresponding antibodies. Fibroblasts (F180 and F184) were included to assess expression in normal cells. Lysates from 40 000 cells were loaded per lane, lysate from SAS cells served as internal standard and actin detection as control. B, Western blot (WB) of UT-SCC 2 and UT-SCC 19A treated with different concentrations of the specific SFK-inhibitor SU6656. The expression and phosphorylation of Src/SFK and the downstream target STAT3 was analyzed using corresponding antibodies. C, Cell proliferation of F184, UT-SCC 2 and UT-SCC 19A treated with increasing concentrations of SFK inhibitor SU6656 for 3 days. The initial cell number was subtracted and the relative cell number is depicted (negative values indicate cell kill). D, Correlation plot: The relative proliferation after 3 days of treatment with 1 µM SU6656 was plotted against the relative SFK phosphorylation (pSFK). pSFK values were obtained from panel (A)

combination approaches such as dual inhibition of SFK and AKT or inhibitor of nuclear factor kappa-B kinase subunit beta (IKKβ)/nuclear factor 'kappa-light-chain-enhancer' of activated B-cells (NF-κB) signaling.[44,45]

Besides SFK we identified other upregulated PTK (eg, members of the erbB, insulin receptor, ROR, Syk and TAM subfamilies). While the erbB subfamily which includes the EGFR is of significant relevance as already outlined above, also other identified PTK subfamilies have

been reported to be overexpressed in HNSCC and might be involved in tumor growth and therapy resistance such as the insulin receptor and ROR subfamily.[46-48] While such former studies analyzed the expression of a certain PTK, the functional profiling used here provides new and complementary insights into the molecular biology of HNSCC. It also highlights the heterogeneity of HNSCC signal transduction, since most alterations were detected only in a small number of patients. If not analyzed in detail already,[20,49,50] the other PTK subfamilies will be tested for potential targetability in separate studies. Notably, we did not identify EGFR hyperactivity in the analyzed samples. However, our analysis does not exclude EGFR activity in the HNSCC. It just demonstrates that there is no increased EGFR activity in HNSCC when compared with the normal epithelial tissue. This is not very surprising, since EGFR is also highly expressed in normal epithelial tissue,[51] and a distinct overexpression is actually less frequent than commonly assumed.[52] Moreover, EGFR expression does not reliably reflect its activity as already discussed above.[7]

In contrast to the relative low variation in the mean overall kinase activity in the tumor tissue group we observed considerable variation in the normal tissue group (Figure S2), with some normal tissues displaying high overall PTK activity which was comparable with the corresponding tumor (#117, #168 and #175; Figure 2B). Interestingly, all these patients had recurrent disease or a high T-stage, suggestive of inflammatory processes or histologically undetectable early premalignant changes in the areas of normal tissue. Through deep sequencing analysis of the remaining normal tissue from #117 and #168 we could indeed detect mutations in p53 (#117, #168) as well as NOTCH1 (#168), which supports this hypothesis (Figure S9). These observations are in line with the concept of field cancerization proposed for HNSCC and are in accordance with previous studies describing increased PTK activity in normal mucosa of tumor patients compared with the mucosa of healthy patients.[53] Together with the high percentage (80%) of HNSCC with strong pSFK score the increased SFK activity in "normal" mucosa also indicates that activation of SFK is an early event in HNSCC development.

One major limitation in the use of fresh specimens in studies such as the one presented here is tissue heterogeneity, for example, the percentage of tumor and normal cells as well as the amount of stroma or extracellular matrix present in a sample. Such discrepancies can be a major problem, especially when comparing normal and tumor tissues, as it can lead to variations in the number of specific cells analyzed at a given protein concentration. To address this problem, we performed single-cell analysis using IHC (see above). Moreover, for half of the samples we cryosectioned the samples before lysis and lysed the sectioned samples in parallel with histological evaluation after hematoxylin-eosin staining (see Section 2.2). We observed no obvious differences concerning the kinome profile or level of kinase activity when comparing this controlled lysis with the uncontrolled lysis performed for the rest of the samples. Furthermore, we also confirmed the results from the upstream kinase analysis using the method of variance stabilizing normalization, which corrects for general imbalances and highlights specific changes. Again, no obvious differences were detectable compared with the standard upstream kinase analysis (data not shown). Nevertheless, controlling the comparability of the used samples by histological evaluation or subsequent single cell analysis using IHC is of great importance when comparing the enzymatic activity in different primary samples. In this study, the verification experiments led to the confirmation of the originally detected changes.

In summary, we present here the first systematic functional analysis of the tyrosine kinome in HNSCC tumors and identify increased SFK activity as a frequent event. In addition to the identification of other highly regulated PTK that provide important new insights into the signal transduction of HNSCC and suggest new potential targets for targeted therapy, this study also shows that functional tests such as kinome profiling may help personalize molecular therapy and thus improve the treatment of cancer.

ACKNOWLEDGMENTS

We greatly acknowledge the technical assistance of Helwe Gerull and the support of all colleagues involved in the sample collection, especially surgeons and nurses of the surgical team. This work was supported by the Federal Ministry of Education and Research (BMBF grant 02NUK032; Malte Kriegs, Kai Rothkamm, Thorsten Rieckmann), the Hamburger Krebsgesellschaft e.V. (Lara Bußmann, Adrian Münscher, Malte Kriegs), the Werner-Otto-Stiftung (Lara Bußmann, Malte Kriegs, Adrian Münscher), the University of Hamburg (Cordula Petersen, Malte Kriegs), the University Cancer Center Hamburg (Malte Kriegs, Conrad Droste), University Cancer Center Hamburg Research Fellowship (Lara Bußmann, Lukas Clemens Böckelmann, Henrike Barbara Zech, Nikolaus Möckelmann, Joanna Caroline Berger), Mildred Scheel Cancer Career Center HaTriCS4 (Lara Bußmann), Stiftung Tumorforschung Kopf-Hals (Joanna Caroline Berger) and the Hamburger Stiftung zur Förderung der Krebsbekämpfung (Lara Bußmann).

CONFLICT OF INTEREST

Savithri Rangarajan and Rik de Wijn are employees of PamGene International B.V. All remaining authors declare no potential conflict of interest.

DATA AVAILABILITY STATEMENT

All experimental results or analyzed during this study are included in this published article. Primary data will be made available upon reasonable request.

ETHICS STATEMENT

Patient samples were collected and processed in accordance with UKE ethical guidelines and regulations, ethical standards of the institutional and/or national research committee, and with the 1964 Helsinki declaration and its later amendments. All patients gave written informed consent.

ORCID

Lara Bußmann https://orcid.org/0000-0001-6302-0859
Konrad Klinghammer https://orcid.org/0000-0001-6425-4833
Malte Kriegs https://orcid.org/0000-0002-6195-8920

REFERENCES

1. Du E, Mazul AL, Farquhar D, et al. Long-term survival in head and neck cancer: impact of site, stage, smoking, and human papillomavirus status. *Laryngoscope*. 2019;129:2506-2513.
2. Kandoth C, McLellan MD, Vandin F, et al. Mutational landscape and significance across 12 major cancer types. *Nature*. 2013;502:333-339.
3. Leemans CR, Braakhuis BJ, Brakenhoff RH. The molecular biology of head and neck cancer. *Nat Rev Cancer*. 2011;11:9-22.
4. Leemans CR, Snijders PJF, Brakenhoff RH. The molecular landscape of head and neck cancer. *Nat Rev Cancer*. 2018;18:269-282.
5. Rieckmann T, Kriegs M. The failure of cetuximab-based de-intensified regimes for HPV-positive OPSCC: a radiobiologists perspective. *Clin Transl Radiat Oncol*. 2019;17:47-50.
6. Bossi P, Resteghini C, Paielli N, Licitra L, Pilotti S, Perrone F. Prognostic and predictive value of EGFR in head and neck squamous cell carcinoma. *Oncotarget*. 2016;7:74362-74379.
7. Kriegs M, Clauditz TS, Hoffer K, et al. Analyzing expression and phosphorylation of the EGF receptor in HNSCC. *Sci Rep*. 2019;9:13564.
8. Cancer Genome Atlas Network. Comprehensive genomic characterization of head and neck squamous cell carcinomas. *Nature*. 2015;517:576-582.
9. Frederick MJ, VanMeter AJ, Gadhikar MA, et al. Phosphoproteomic analysis of signaling pathways in head and neck squamous cell carcinoma patient samples. *Am J Pathol*. 2011;178:548-571.
10. Wu Z, Doondeea JB, Gholami AM, et al. Quantitative chemical proteomics reveals new potential drug targets in head and neck cancer. *Mol Cell Proteomics*. 2011;10:M111.011635.
11. Moser R, Xu C, Kao M, et al. Functional kinomics identifies candidate therapeutic targets in head and neck cancer. *Clin Cancer Res*. 2014;20:4274-4288.
12. Munscher A, Prochnow S, Gulati A, et al. Survivin expression in head and neck squamous cell carcinomas is frequent and correlates with clinical parameters and treatment outcomes. *Clin Oral Investig*. 2019;23:361-367.
13. Simon R, Mirlacher M, Sauter G. Immunohistochemical analysis of tissue microarrays. *Methods Mol Biol*. 2010;664:113-126.
14. Huber W, Carey VJ, Gentleman R, et al. Orchestrating high-throughput genomic analysis with Bioconductor. *Nat Methods*. 2015;12:115-121.
15. Therneau MT, Grambsch MP. *Modeling Survival Data: Extending the Cox Model*. New York: Springer; 2000.
16. Kassambara A, Kosinski M. *survminer: Drawing Survival Curves using "ggplot2." R Package Version 0.4.3*. 2018. https://github.com/kassambara/survminer.
17. Wickham H. Reshaping data with the reshape package. *J Stat Softw*. 2007;21:1-20.
18. Wei A, Simko V. *R Package "Corrplot": Visualization of a Correlation Matrix (Version 0.84)*. 2017. https://github.com/taiyun/corrplot.
19. Jääskelä-Saari HA, Kairemo KJ, Jekunen AP, et al. Cytotoxicity of bleomycin and external radiation in squamous cell cancer cell lines of head and neck. *Cancer Detect Prev*. 1996;20:279-284.
20. Kasten-Pisula U, Saker J, Eicheler W, et al. Cellular and tumor radiosensitivity is correlated to epidermal growth factor receptor protein expression level in tumors without EGFR amplification. *Int J Radiat Oncol Biol Phys*. 2011;80:1181-1188.
21. Kriegs M, Kasten-Pisula U, Riepen B, et al. Radiosensitization of HNSCC cells by EGFR inhibition depends on the induction of cell cycle arrests. *Oncotarget*. 2016;7:45122-45133.
22. Arni S, Le THN, de Wijn R, et al. Ex vivo multiplex profiling of protein tyrosine kinase activities in early stages of human lung adenocarcinoma. *Oncotarget*. 2017;8:68599-68613.
23. Nollau P, Mayer BJ. Profiling the global tyrosine phosphorylation state by Src homology 2 domain binding. *Proc Natl Acad Sci USA*. 2001;98:13531-13536.
24. Eid S, Turk S, Volkamer A, Rippmann F, Fulle S. KinMap: a web-based tool for interactive navigation through human kinome data. *BMC Bioinformatics*. 2017;18:16.
25. Khan SA, Tyagi M, Sharma AK, et al. Cell-type specificity of beta-Actin expression and its clinicopathological correlation in gastric adenocarcinoma. *World J Gastroenterol*. 2014;20:12202-12211.
26. Irby RB, Yeatman TJ. Role of Src expression and activation in human cancer. *Oncogene*. 2000;19:5636-5642.
27. Martin GS. The hunting of the Src. *Nat Rev Mol Cell Biol*. 2001;2:467-475.
28. Wheeler DL, Iida M, Dunn EF. The role of Src in solid tumors. *Oncologist*. 2009;14:667-678.
29. Martin D, Abba MC, Molinolo AA, et al. The head and neck cancer cell oncogenome: a platform for the development of precision molecular therapies. *Oncotarget*. 2014;5:8906-8923.
30. van Oijen MG, Rijksen G, ten Broek FW, Slootweg PJ. Overexpression of c-Src in areas of hyperproliferation in head and neck cancer, premalignant lesions and benign mucosal disorders. *J Oral Pathol Med*. 1998;27:147-152.
31. Mao L, Deng WW, Yu GT, et al. Inhibition of SRC family kinases reduces myeloid-derived suppressor cells in head and neck cancer. *Int J Cancer*. 2017;140:1173-1185.
32. Zhang Q, Thomas SM, Xi S, et al. SRC family kinases mediate epidermal growth factor receptor ligand cleavage, proliferation, and invasion of head and neck cancer cells. *Cancer Res*. 2004;64:6166-6173.
33. Xi S, Zhang Q, Dyer KF, et al. Src kinases mediate STAT growth pathways in squamous cell carcinoma of the head and neck. *J Biol Chem*. 2003;278:31574-31583.
34. Johnson FM, Saigal B, Talpaz M, Donato NJ. Dasatinib (BMS-354825) tyrosine kinase inhibitor suppresses invasion and induces cell cycle arrest and apoptosis of head and neck squamous cell carcinoma and non-small cell lung cancer cells. *Clin Cancer Res*. 2005;11:6924-6932.
35. Ammer AG, Kelley LC, Hayes KE, et al. Saracatinib impairs head and neck squamous cell carcinoma invasion by disrupting Invadopodia function. *J Cancer Sci Therapy*. 2009;1:52-61.
36. Brooks HD, Glisson BS, Bekele BN, et al. Phase 2 study of dasatinib in the treatment of head and neck squamous cell carcinoma. *Cancer*. 2011;117:2112-2119.
37. Fury MG, Baxi S, Shen R, et al. Phase II study of saracatinib (AZD0530) for patients with recurrent or metastatic head and neck squamous cell carcinoma (HNSCC). *Anticancer Res*. 2011;31:249-253.
38. Bauman JE, Duvvuri U, Gooding WE, et al. Randomized, placebo-controlled window trial of EGFR, Src, or combined blockade in head and neck cancer. *JCI Insight*. 2017;2:e90449.
39. Purnell PR, Mack PC, Tepper CG, et al. The Src inhibitor AZD0530 blocks invasion and may act as a radiosensitizer in lung cancer cells. *J Thorac Oncol*. 2009;4:448-454.
40. Tryfonopoulos D, Walsh S, Collins DM, et al. Src: a potential target for the treatment of triple-negative breast cancer. *Ann Oncol* 2011;22: 2234–40.
41. Stegeman H, Span PN, Rijken PF, et al. Dasatinib inhibits DNA repair after radiotherapy specifically in pSFK-expressing tumor areas in head and neck xenograft tumors. *Trans Oncol* 2013;6: 413–9.
42. Yu GT, Mao L, Wu L, et al. Inhibition of SRC family kinases facilitates anti-CTLA4 immunotherapy in head and neck squamous cell carcinoma. *Cell Mol Life Sci*. 2018;75:4223-4234.
43. Lang L, Shay C, Xiong Y, et al. Combating head and neck cancer metastases by targeting Src using multifunctional nanoparticle-based saracatinib. *J Hematol Oncol*. 2018;11:85.

44. Lang L, Shay C, Zhao X, Xiong Y, Wang X, Teng Y. Simultaneously inactivating Src and AKT by saracatinib/capivasertib co-delivery nanoparticles to improve the efficacy of anti-Src therapy in head and neck squamous cell carcinoma. *J Hematol Oncol*. 2019;12:132.
45. Yang Z, Liao J, Cullen KJ, Dan H. Inhibition of IKKβ/NF-κB signaling pathway to improve Dasatinib efficacy in suppression of cisplatin-resistant head and neck squamous cell carcinoma. *Cell Death Dis*. 2020;6:36.
46. Barnes CJ, Ohshiro K, Rayala SK, El-Naggar AK, Kumar R. Insulin-like growth factor receptor as a therapeutic target in head and neck cancer. *Clin Cancer Res*. 2007;13:4291-4299.
47. Khalil A, Jameson MJ. Downregulation of IGF1R expression inhibits growth and enhances cisplatin sensitivity of head and neck squamous cell carcinoma cells in vitro. *Hormones Cancer*. 2019;10:11-23.
48. Zhang W, Yan Y, Gu M, et al. High expression levels of Wnt5a and Ror2 in laryngeal squamous cell carcinoma are associated with poor prognosis. *Oncol Lett*. 2017;14:2232-2238.
49. Kriegs M, Gurtner K, Can Y, et al. Radiosensitization of NSCLC cells by EGFR inhibition is the result of an enhanced p53-dependent G1 arrest. *Radiother Oncol*. 2015;115:120-127.
50. Myllynen L, Kwiatkowski M, Gleissner L, et al. Quantitative proteomics unveiled: regulation of DNA double strand break repair by EGFR involves PARP1. *Radiother Oncol*. 2015;116:423-430.
51. Gusterson BA, Hunter KD. Should we be surprised at the paucity of response to EGFR inhibitors? *Lancet Oncol*. 2009;10:522-527.
52. Khaznadar SS, Khan M, Schmid E, et al. EGFR overexpression is not common in patients with head and neck cancer. Cell lines are not representative for the clinical situation in this indication. *Oncotarget*. 2018;9:28965-28975.
53. Verschuur HP, Rijksen G, Schipper-Kester GP, et al. Protein tyrosine kinase activity in laryngeal squamous cell carcinoma. *Eur Arch Oto-Rhino-Laryngol*. 1993;249:466-469.

SUPPORTING INFORMATION

Additional supporting information may be found online in the Supporting Information section at the end of this article.

How to cite this article: Bußmann L, Hoffer K, von Bargen CM, et al. Analyzing tyrosine kinase activity in head and neck cancer by functional kinomics: Identification of hyperactivated Src family kinases as prognostic markers and potential targets. *Int. J. Cancer*. 2021;1–15. https://doi.org/10.1002/ijc.33606